Contribution of Reactive Oxygen Species to Thymineless Death in *Escherichia coli*

Yuzhi Hong[1], **Liping Li**[1], **Gan Luan**[1], **Karl Drlica**[1], and **Xilin Zhao**[1,2,*]

[1]Public Health Research Institute and Department of Microbiology, Biochemistry & Molecular Genetics, New Jersey Medical School, Rutgers University, 225 Warren Street, Newark, NJ 07103

[2]State Key Laboratory of Molecular Vaccinology and Molecular Diagnostics, School of Public Health, Xiamen University, South Xiang-An Road, Xiang-An District, Xiamen, Fujian Province, 361102, China

Keywords

thymineless death (TLD); reactive oxygen species (ROS); respiratory chain; antioxidant; single-stranded DNA gaps; double-stranded DNA breaks

Introductory paragraph

Nutrient starvation usually halts cell growth rather than causing death. Thymine starvation is exceptional, because it rapidly kills cells. This phenomenon, called thymineless death (TLD), underlies the action of several antibacterial, antimalarial, anticancer, and immunomodulatory agents. Many explanations for TLD have been advanced, with recent efforts focused on recombination proteins and replication origin (*oriC*) degradation. Since current proposals account for only part of TLD and since reactive oxygen species (ROS) are implicated in bacterial death due to other forms of harsh stress, we investigated possible involvement of ROS in TLD. Here we show that thymine starvation led to accumulation of both single-strand DNA regions and intracellular ROS; interference with either event protected bacteria from double-strand DNA breakage and TLD. Elevated levels of single-strand DNA were necessary but insufficient for TLD, while reduction of ROS to background levels largely abolished TLD. We conclude that ROS contribute to TLD by converting single-stranded DNA lesions into double-stranded DNA breaks. Participation of ROS in the terminal phases of TLD provides a specific example for how ROS contribute to stress-mediated bacterial self-destruction.

*Correspondence and requests for materials: Xilin Zhao (zhaox5@njms.rutgers.edu).

When cells are starved for nutrients (amino acids, nucleotides, or vitamins), growth usually stops until the nutrient becomes available [1]. Starvation for thymine or thymidine (T-starvation) is different -- cells die rapidly [2,3]. Both prokaryotic and eukaryotic cells exhibit this phenomenon known as thymineless death (TLD) [1]. The mechanism of TLD is of considerable interest, because it underlies the effectiveness of several antibacterial (trimethoprim, sulfamethoxazole), antimalarial (pyrimethamine, sulfonamide), anticancer (methotrexate, fluorouracil), and immune-modulating (methotrexate) agents. Proposed explanations for TLD have included unbalanced growth [2], toxin-antitoxin module action [4], nucleotide mis-incorporation [5], induction of the SOS regulon[6], and destruction of replication forks [7–9]. Previous work also focused on recombination events, some of which are protective and some of which are destructive [6,9–11]. Recent studies suggested that TLD in *Escherichia coli* derives from the degradation of the replication origin (*oriC*) [6,12–15]. However, *oriC* copy number, relative to that of the replication terminus, fails to drop below unity [6,12,14], indicating an incomplete loss of *oriC*. The remaining *oriC* should be sufficient for viability when thymine becomes available for recombinational repair. Moreover, a counter-example occurs with a *thyA-recBC* double mutant in which preferential loss of *oriC* is eliminated, but death due to T-starvation is not [14]. Overall, previous work does not explain why genetic perturbations only partially block the death process; moreover, some explanations are weakened by counter-arguments [1,16–18]. Thus, additional work is needed to understand events involved in TLD.

Among the unexplained observations is a reduction in TLD by deficiencies in the recombination genes *recQ* and *recF* [6,11,19,20]. The wild-type products may be destructive during T-starvation by increasing single-stranded DNA (ssDNA) regions [7,21]. Since double-strand DNA breaks (DSBs) are involved in TLD [9,14,22], ssDNA regions/lesions, enlarged by RecF and RecQ, may serve as substrates for DNA breakage as part of a self-destructive response to stress. Work with antimicrobials indicates that some destructive stress responses involve reactive oxygen species (ROS)[23–26]; in the case of TLD, persistent ssDNA regions/lesions [14] may be substrates for production of lethal DSBs by ROS.

The present work used three strategies to examine the role of ROS in TLD. One interfered with ROS accumulation by inhibiting hydroxyl radical production/accumulation using chemical inhibitors. A second examined effects of mutations in genes that normally influence ROS levels or the accumulation of ssDNA regions. The third approach used flow cytometry to monitor ROS and fluorescence microscopy to measure the prevalence of *E. coli* cells containing elevated ROS levels, ssDNA regions, and DSBs, each of which accumulated during T-starvation of cells grown in a defined, nutrient-rich medium. Single-stranded DNA regions/lesions were necessary but insufficient for TLD, an observation that was consistent with their conversion into lethal DSBs by ROS.

Results

ROS are associated with TLD

To monitor ROS level, we examined the fluorescence of ROS-sensitive dyes. Removal of thymidine from cultures of an *E. coli* thymidylate synthetase mutant (*thyA*) increased intracellular ROS, monitored by flow cytometry (Fig. 1a) and by fluorescence microscopy

(Supplementary Fig. 1a) using carboxy-H2DCFDA, a fluorescent, ROS indicator dye. The surge in intracellular ROS paralleled cell death (compare Fig. 1a,b and Supplementary Fig. 1b). Moreover, a dye specific for hydrogen peroxide, Peroxy Orange-1, revealed accumulation of H_2O_2 during TLD (Fig. 1c and Supplementary Fig. 1c). T-starvation also increased lipid peroxidation, as indicated by fluorescence of C11-BODIPY, a dye specific for lipid peroxidation (Fig. 1d and Supplementary Fig. 1d). Control experiments showed very low ROS accumulation by either wild-type cells growing without thymidine or by the *thyA* mutant growing in medium containing thymidine (Supplementary Fig. 1e-h). Moreover, auto-fluorescence contributed little to our measurements, as cells having no dye showed no background fluorescence during microscopy and a much lower fluorescence intensity upshift in flow cytometry than when dye was present (Supplementary Fig. 2). Thus, an increase in ROS accompanies TLD.

We next perturbed ROS levels. Agents that inhibit ROS accumulation, such as the iron chelator 2,2'-bipyridyl [23,27] or the hydroxyl-radical scavenger dimethyl sulfoxide (DMSO) [28], reduced both ROS accumulation and TLD (Fig. 1b and Supplementary Fig. 3a-c). Conversely, deletion of peroxide-detoxifying genes, such as *katG/E*, generated a hyperlethal phenotype during T-starvation (Fig. 1e and Supplementary Figs. 3d, 4a). We performed the latter experiment with minimal medium, because the higher ROS levels in rich medium (Supplementary Fig. 3e-h) would mask the added effect of a catalase deficiency (Supplementary Fig. 3d). Two additional experiments supported involvement of ROS in TLD. First, when trimethoprim triggered TLD, lethal action was reduced by DMSO and exacerbated by a deficiency in *katG* (Supplementary Fig. 4a). Second, when a *thyA* mutant growing anaerobically was starved for thymidine, TLD was lowered; it was eliminated by additional treatment with bipyridyl (Supplementary Fig. 4b). Thus, TLD is associated with a surge in ROS, reduced by agents that inhibit ROS accumulation, and enhanced by deficiencies in genes that protect from ROS.

Respiratory genes are involved in ROS accumulation and TLD

General inhibitors of RNA and protein synthesis (rifampicin and chloramphenicol) abolish TLD [13,29,30], but the underlying mechanism is poorly understood due to pleiotropic effects of these agents. Since both drugs reduce cellular respiration [31], and since ROS are normal by-products of respiration, we expected these inhibitors to block TLD in part by suppressing ROS accumulation. Indeed, the surge in ROS associated with T-starvation was reduced by rifampicin and chloramphenicol (Fig. 2a,b).

We also asked whether particular respiratory proteins participate in ROS accumulation and TLD. In *E. coli*, ubiquinone transfers electrons from multiple input dehydrogenases to three output terminal oxidases (cytochromes *bd-I, bd-II*, and *bo* [32]). Deletion of *ubiG*, a gene required for ubiquinone biosynthesis, decreased ROS accumulation and enhanced survival during T-starvation (Fig. 2c,d). Inactivation of *bd-I* oxidase (*cydB*) also reduced ROS accumulation and TLD (Fig. 2c-d). To attribute the reduction in TLD to deficiencies in *ubiG* and *cydB*, we showed that plasmid-borne copies of the wild-type genes restored *thyA*-mediated TLD (Supplementary Fig. 5a,b). Disruption of the other terminal oxidases, AppBC (*bd-II* oxidase) or CyoABCDE (*bo* oxidase), or several of the many electron-input enzymes

(succinate dehydrogenase or NADH dehydrogenases I or II), individually had no effect on either ROS accumulation or TLD (Supplementary Fig. 5c-f). Thus, *bd-1* oxidase is the major terminal oxidase responsible for the correlation of ROS production with TLD. These data fit with respiratory proteins contributing to TLD and support ROS involvement in TLD.

Since a deficiency of *ubiG* or *cydB* only partially eliminated the ROS surge or TLD, we next added bipyridyl to the *thyA- ubiG* culture to further reduce ROS. This treatment reduced ROS to background levels and largely abolished TLD, even after prolonged (5 h) T-starvation (Fig. 2d and Supplementary Fig. 6a,b). Thus, ROS are the dominant source of TLD. The contribution of other cellular activities, such as replication, transcription, and toxic recombination/repair, to TLD is likely through ROS-mediated events, since each is expected to persist in bipyridyl treated *thyA- ubiG* cultures in which neither ROS accumulation nor TLD occur.

Accumulation of single-stranded DNA is necessary but insufficient for TLD

During TLD, bacterial chromosomes are expected to accumulate regions of single-stranded DNA in lagging strands of replication forks and at sites of single-stranded lesion repair. Indeed, single-stranded DNA lesions are observed during thymine starvation [22]. Due to the absence of dTTP, these ssDNA regions/lesions cannot be filled and will tend to persist [14]. The role of ssDNA regions in TLD can be studied using deficiencies in RecQ and RecFOR recombinational repair, since these proteins are thought to generate/expand ssDNA regions [7,21,33]; moreover, deficiencies in *recQ* and *recF* protect from TLD [11,19,20]. Deletion of *recF* or *recR* delayed TLD onset by about 45 min (Fig. 3a). Deletion of *recQ* had a greater effect: killing decreased by ~300 fold after 3 h of starvation (Fig. 3b). Thus, ssDNA regions/lesions appear to contribute to TLD.

To obtain direct evidence for accumulation of ssDNA regions during T-starvation, we performed fluorescence microscopy with cells expressing a plasmid-borne gene encoding single-strand DNA-binding protein (Ssb) fused to yellow fluorescent protein (YFP). Fluorescent foci were detected 30 min after starvation (Fig. 3c). Auto-fluorescence did not interfere with such measurements, since cells lacking Ssb-YFP expression were completely dark (Supplementary Fig. 2a) and since cells expressing Ssb-YFP in the presence of thymidine displayed a weak, uniform background fluorescence without foci (Fig. 3c-f, time-zero images). As expected [21,34], a double deficiency in *recQ* and *thyA* lowered the prevalence of cells with ssDNA regions during T-starvation. For example, starvation for 30 min increased the prevalence of *thyA* cells having Ssb-YFP fluorescent foci from <1% to >95% (Fig. 3c), while removal of *recQ* from the *thyA* mutant reduced the prevalence of foci (none was seen even after 60 min of starvation (Fig. 3d)).

We also examined a deficiency of *rnhA* (RNase HI). This ribonuclease degrades RNA in RNA-DNA hybrids (R-loops) formed during transcription [35] and can participate in removal of RNA primers associated with lagging-strand DNA synthesis [36,37]. Both processes are expected to increase levels of ssDNA regions [38], and indeed a deficiency in *rnhA* reduced TLD (Fig. 3b). Deletion of *rnhA*, when combined with the *thyA* mutation, also suppressed formation of ssDNA regions, since the number of fluorescent foci was reduced after T-starvation for 30 min. However, the reduction was not as great as seen with a *recQ* defect:

after starvation for 60 min, ~50% of the *rnhA*- *thyA* double mutant cells exhibited fluorescent foci (Fig. 3e), while for the *recQ*- *thyA* mutant the prevalence of foci was <5% (Fig. 3d). Additional work is required to determine whether RNA-DNA hybrids, apart from generation of ssDNA regions at replication forks, contribute to TLD.

Collectively, the data indicate that mutations expected to protect from TLD by reducing ssDNA regions lower the prevalence of cells exhibiting fluorescent foci originating from regions of single-stranded DNA. Conversely, mutations that protect from TLD by suppressing ROS accumulation (such as *cydB*) had no effect on the prevalence of cells showing ssDNA regions (Fig. 3f and Supplementary Fig. 7a).

Since both ROS and ssDNA regions are involved in TLD and since rifampicin reduces ROS accumulation (Fig. 2a) and blocksTLD [13,29,39], we next examined the effect of rifampicin on the accumulation of ssDNA regions during T-starvation. Rifampicin had little effect on the prevalence of cells containing Ssb-YFP fluorescent foci (Fig. 3g and Supplementary Fig. 7a,b). Likewise, treatment with 2,2'-bipyridyl, which suppresses the accumulation of ROS, had little effect on Ssb-YFP foci (Supplementary Figs. 3a, 7c). Thus, single-stranded DNA is required for TLD, but it is insufficient (rifampicin blocks TLD but not formation of ssDNA regions). Since rifampicin also blocks initiation of replication [15,40] and transcription [41], the data in Fig. 3g indicate that replication and transcription initiation are not required for the accumulation of ssDNA regions during T-starvation.

Conversion of single-stranded DNAs into DNA breaks by ROS underlies TLD

Requiring both ssDNA regions and ROS for TLD fits with the ability of ROS to produce mostly non-lethal, single-strand DNA cleavage when attacking double-stranded DNA [42]. Only in the rare situation in which two nearby attacks occur, one in each of the two complementary DNA strands, would a double-stranded break arise (illustrated in Supplementary Fig. 8a). However, ROS attack at ssDNA regions would readily produce DSBs. Thus, an increase in size and/or number of ssDNA regions would increase the production of ROS-mediated DSBs, which may be a major cause of TLD.

Although early work correlated DSB and TLD [9,14,22], a more recent study suggested that rifampicin might inhibit TLD without blocking DNA breakage [13]. Such a conclusion would undermine the idea that DSBs cause TLD. Consequently, we reinvestigated relationships between DNA breakage and TLD by performing a single-cell assay in which a fusion of *E. coli* RecN and yellow fluorescent protein (YFP) was used to measure the prevalence of cells having DSBs (detection by *E. coli* RecN-YFP was similar to detection by a well-characterized *B. subtilis* RecN-YFP; Supplementary Fig. 9). With the *thyA* mutant growing in thymidine-containing medium or with wild-type cells cultured in thymidine-depleted medium, the prevalence of cells showing RecN-YFP-mediated fluorescent foci was low (<0.1%; Supplementary Fig. 8b). In contrast, T-starvation for 60 min caused almost all *thyA* cells (95%) to exhibit at least one RecN-YFP focus (Fig. 4a). Rifampicin treatment reduced the number of RecN-YPF foci to ~18% (Fig. 4b) while inhibiting cell death (Supplementary Fig. 8c). Likewise, treatment of starved cells with 2,2'-bipyridyl, which reduces ROS accumulation and TLD (Fig. 1b and Supplementary Fig. 3a), also suppressed DNA breakage (Fig. 4c). Thus, DSBs and an ROS surge correlate with TLD.

Involvement of ssDNA regions in DNA breakage and TLD was also observed when the prevalence of cells with DNA breaks was examined using a *thyA- recQ* double mutant. While 60 min of T-starvation with the *thyA* mutant allowed approximately 95% of the cells to exhibit DSBs (Fig. 4a), an additional deficiency in *recQ* reduced the number to below 5% (Fig. 4d) and increased survival (Fig. 3b). In summary, reduction in either ROS or ssDNA regions lowers DNA breakage and TLD, but reduction of ROS has little effect on formation of ssDNA regions (Fig. 3f,g and Supplementary Fig. 7), indicating that ROS do not affect TLD through reduced accumulation of ssDNA regions.

To test the idea that DNA breaks occur in regions of single-stranded DNA, we used fluorescence microscopy to examine co-localization of RecN, which reveals DSBs, and Ssb, which associates with single-stranded DNAs. When we monitored the same thymidine-starved *thyA* cells by microscopy over time, intense Ssb-mCherry foci (ssDNA regions) started to appear 20 min after initiation of starvation (Fig. 4e), consistent with our earlier observation of ssDNA accumulation (Fig. 3c). RecN-YFP foci (DSBs) appeared at least 30 min later (Fig. 4a,e), and newly formed breaks co-localized with ssDNA regions (Fig. 4e). Analysis of more than 30 newly formed RecN-YFP foci showed that ~60% of the breaks co-localized with single-strand DNA regions. Thus, DNA breaks associated with TLD tend to occur at ssDNA regions, as expected from the known action of ROS [42].

We also expected that administering exogenous peroxide would overcome the protection from TLD afforded by reduced production of endogenous ROS. As a test, we first accumulated ssDNA regions by treating thymidine-starved *thyA*-deficient cells with rifampicin for 30 min, which suppressed accumulation of endogenous ROS (Fig. 2a) and eliminated TLD (Supplementary Figs. 8c, 10a) but allowed formation of ssDNA regions (Fig. 3g). Then we treated for an additional 20 min with exogenous H_2O_2 at a concentration that was non-lethal for wild-type cultures or for *thyA* cultures supplemented with thymidine (Supplementary Fig. 10b). Exogenous H_2O_2 reduced survival of thymidine-starved, rifampicin-treated *thyA* cells from 100% to below 0.1% (Fig. 5a). The exogenous H_2O_2 treatment of thymidine-starved *thyA* cells also raised the fraction of cells having DNA breaks (RecN-YFP foci) from about 18% to 75% (Fig. 5b,c). When thymidine was present, H_2O_2 did not trigger a surge in DNA breaks in the *thyA* mutant (Fig. 5b,c). Collectively these data support the conclusion that conversion of single-strand DNA regions into breaks by endogenous ROS is a major cause of TLD.

If TLD derives from ROS-mediated conversion of ssDNA regions into DSBs, exogenous H_2O_2-mediated killing should be mitigated by perturbations that reduce the number and/or size of ssDNA regions. Indeed, deficiencies in *recQ* and *rnhA* protected *E. coli* from exogenous peroxide-mediated killing of rifampin-treated, thymidine-starved cultures (Fig. 5d and Supplementary Fig. 10c). In contrast, mutants deficient in genes such as *cydB* and *ubiG*, which reduce intracellular ROS but not ssDNA regions, allowed killing by exogenous peroxide (Figs. 2c, 3f, 5d and Supplementary Fig. 10d). These observations fit with ROS converting elevated levels of persistent ssDNA regions, arising from T-starvation, into DSBs associated with rapid cell death.

The temporal order of appearance of ssDNA regions, ROS, DSBs, and cell death also supports TLD arising from ROS-mediated breakage of DNA in ssDNA regions -- accumulation of ssDNA regions was seen at 30 min of T-starvation, whereas the ROS surge, DSBs, and death were not obvious until 60 min (Supplementary Fig. 11). DNA breaks and the ROS surge appeared at the same time, and both continued to accumulate as survival decreased; in contrast, ssDNA regions tended to saturate after 30 min of starvation (Supplementary Fig. 11).

Discussion

The work described above adds ROS to explanations of TLD. Two pathways (Fig. 6) converge to generate lethal double-strand DNA breaks. In one, T-starvation leads to persistent single-strand DNA regions/lesions that are expanded by RecF and RecQ. In the other, an undefined signal stimulates ROS accumulation; elevated levels of ROS then convert single-strand DNA into DNA breaks. Attempts to repair breaks involve genes, such as *recBC* and *ruvABC*, that, when deficient, render cells hypersensitive to T-starvation [6,9,11,14]; moreover, RecA/RecFOR-mediated toxic recombination may occur [6,9,10], which can be mitigated by UvrD antagonizing RecAFOR function [9,11]. As pointed out above, RecQ/RecFOR may facilitate TLD by promoting/expanding ssDNA regions that serve as substrates for ROS-mediated lethal DSB production. Induction of the SOS response would then activate the SulA checkpoint that blocks cell growth on thymine-containing agar during survival measurement [6]. A double deficiency of *mutM* and *mutY*, genes that are responsible for removal of 8-oxo-dGTP [43], showed a 2–4 fold protection from TLD, while overexpression of *mutT* (encoding an 8-oxo-dGTP sanitizer) exhibited little protection (Supplementary Fig. 12), unlike the large protective effect observed with antimicrobial killing [43]. Several other repair genes, such as *ung, uvrA*, and *mutS* [9,11], showed no effect. Collectively, these data suggested that excision of incorrect or damaged bases has at most a minor contribution to TLD.

Several lines of work support the two pathways in Fig. 6. First, accumulation of ROS is lowered and TLD is blocked/reduced by treatment with rifampicin, chloramphenicol, an iron chelator, a radical scavenger, and deletion of respiratory genes. Second, deficiencies in enzymes that normally reduce levels of peroxide increase the rate and extent of TLD. Third, regions of single-strand DNA persist when replication is halted by T-starvation [22] and are likely expanded by RecF and RecQ [7,21,33]; RNaseH, which generates single-stranded regions of DNA [38], also contributes to TLD. Other potential sources of single-stranded DNA involve attempts to repair nicks created by a variety of sources (e.g. ROS [44], transcription [45], base misincorporation [18], and base oxidization [43]). Fourth, DNA breaks co-localize with regions of single-strand DNA, and sublethal exogenous H_2O_2 becomes lethal under conditions that allow T-starvation to accumulate ssDNA lesions but an insufficient level of endogenous ROS. Finally, TLD was largely abolished when ROS was reduced to background levels by a respiratory deficiency plus either an iron chelator or *recF* (Fig. 2d and supplementary Fig. 6). Thus, most, if not all, of TLD depends on ROS under nutrient-rich conditions.

The inhibitory effects of rifampicin on TLD are complex. Since this drug inhibits transcription and TLD, an argument can be made that during T-starvation transcription converts ssDNA regions to DSBs. However, transcription cannot be sufficient for TLD, since it is expected to occur even when TLD is largely blocked by bipyridyl treatment of a *thyA-ubiG* mutant or by combination of *thyA* with *cydB* and *recF* during T-starvation. Another issue is that our *in vivo* single-cell-based microscopy study showed that rifampicin inhibits DNA breakage, which contradicts previous work using a batch culture-based gel electrophoresis assay [13]. The latter assay suffers from technical ambiguities. For example, T-starvation may generate complex DNA structures [7,46] that might not form during rifampicin treatment [47], thereby allowing rifampicin-treated samples to enter the gel more readily than rifampicin-untreated ones. Another feature of rifampicin is its inability to block the accumulation of ssDNA regions during T-starvation. Even though rifampicin blocks initiation of replication and transcription [15,40,41], it does not block death from concentrations of exogenous peroxide that are normally non-lethal. Thus, initiation of replication or transcription is not required for accumulation of ssDNA regions or TLD when cells are grown in nutrient-rich medium.

We consider TLD to be an example of bacterial self-destruction that occurs when stress is severe. The process is an active one, since transcription, translation, and DNA-damage repair systems are involved [1,6,9,11,14,18]. Other examples of self-destruction include part of the lethal activity associated with diverse antimicrobials [23,25,26]. With antimicrobial-mediated killing, a pathway to ROS accumulation is thought to include toxin-antitoxin (TA) modules (e.g. MazEF), the two-component CpxAR and ArcAB systems, a small regulatory RNA (tmRNA, encoded by *ssrA*), and the ClpAP protease [25,26,48,49]. However, ROS and TLD are unaffected by the absence of TA modules (Supplementary Fig. 13a-d); moreover, disruption of *arcA/B, lon, clpA/P, cpxA/R*, or *ssrA* has little effect on TLD (Supplementary Fig. 13e-i). Thus, the pathways to TLD and antimicrobial-mediated death differ in how they elicit ROS accumulation. Nevertheless, surges in ROS and involvement of the respiratory chain are shared features [23,31,50], as is the presence of metabolically inert, persister subpopulations that tolerate many types of lethal stress. The next challenge is to learn how bacterial cells sense the macromolecular lesions that stimulate a self-destructive ROS surge.

Methods and Materials

Bacterial strains, growth conditions, and reagents

E. coli strains (Supplementary Table 1) were grown aerobically in Hi-DEF Azure medium (Teknova, Hollister, CA) or in M9 minimal medium with 1% glucose, both with 50 μg ml^{-1} thymidine at 37 °C unless specified otherwise. Thermo Fisher Scientific Corp. (Waltham, MA) supplied ROS-sensitive dyes: *5(6)*-carboxy-2',7'-dichlorodihydrofluorescein diacetate (Carboxy-H2DCFDA, which penetrates cells in its parental form but cannot exit the cell once the compound is cleaved by cellular esterases [51]), 2',3',6',7'-tetrahydro-12'-(4,4,5,5-tetramethyl-1,3,2-dioxaborolan-2-yl)-spiro[isobenzofuran-1(3H),9'-[1H,5H,9H]xantheno[2,3,4-ij]quinolizin]-3-one (Peroxy Orange-1), and 4,4-difluoro-5-(4-phenyl-1,3-butadienyl)-4-bora-3a,4a-diaza-s-indacene-3-undecanoic acid (C11-BODIPY). Other reagents were from Sigma-Aldrich Corp. (St. Louis, MO).

Thymidine starvation and bacterial survival measurement

Overnight cultures were diluted 200-fold into fresh medium, grown to log phase (A_{600} = 0.15) with rotary shaking at 250 rpm, collected by centrifugation (8,000 g for 30 s), and washed with the same volume of saline (0.9% NaCl) at room temperature to remove thymidine. Cell pellets from 1-ml cultures were suspended in 2 ml fresh medium lacking thymidine. When appropriate, 2,2'-bipyridyl or DMSO was added to a final, sub-inhibitory concentration of 0.35 mM or 700 mM (0.5 × MIC), respectively. Cultures were immediately shifted to 37 °C with shaking to initiate T-starvation. All survival data were normalized to cell density (2 to 5×10^7 CFU ml^{-1}) at the time starvation was initiated to facilitate comparisons of experiments.

For TLD during anaerobiosis, the *thyA* mutant was grown in Hi-DEF Azure medium containing 50 mM fumarate and 50 μg ml^{-1} thymidine in a sealed Vacutainer blood-draw tube (BD Medical Supplies, Franklin Lakes, NJ) through which Bioblend anaerobic gas (10% H_2, 5% CO_2, 85% N_2 (Welco Gas Corp., Newark, NJ)) was passed for 30 min via a long inlet needle submerged in the medium and a short outlet needle at the top of the head space of the tube. Both needles passed through the rubber stopper of the Vacutainer tube, which was sealed when the needles were removed. When the culture density reached A_{600} of 0.15, cells were concentrated by centrifugation, resuspended in medium lacking thymidine, and pre-treated with Bioblend anaerobic gas in a Vacutainer tube for 30 min. Aliquots were removed via syringe through the inlet needle, diluted in saline containing 50 μg ml^{-1} thymidine, applied to LB agar containing thymidine, and incubated overnight in ambient air to determine CFU.

H_2O_2 was used to overcome the inhibitory effect of rifampicin on TLD by growing bacteria to A_{600} = 0.15 in Hi-DEF Azure medium with 50 μg ml^{-1} thymidine, adding rifampin to 5 × MIC (50 μg ml^{-1}) when cells were suspended in fresh medium lacking thymidine, and at various times adding H_2O_2 to 3.5 mM. After H_2O_2 treatment for 20 min, aliquots were removed for CFU determination.

Flow cytometry

Bacterial fluorescence intensity was determined using fluorescence-based flow cytometry. Carboxy-H2DCFDA (10 μM), Peroxy Orange-1 (5 μM), or C11-BODIPY (2 μM) was present in the growth medium to detect overall intracellular ROS, H_2O_2, or lipid peroxidation, respectively [51–53]. A no-dye sample was included to control for auto-fluorescence. A total of 100,000 ungated events for each time-point sample was determined by a BD Accuri C6 Plus flow cytometer (Becton Dickinson, USA) using the following detection parameters: 20 mV laser power, 533/30 nm band pass filter (FL1-channel) for Carboxy-H2DCFDA, and 585/40 nm band pass filter (FL2-channel) for Peroxy Orange-1 and C11-BODIPY. Data were analyzed using the BD Accuri C6 software.

Visualization of DNA lesions

E. coli cells containing single- or double-strand DNA breaks were detected by fluorescence microscopy using yellow fluorescent protein (YFP) fused to single-strand DNA-binding protein (Ssb) or RecN. The ability of *E. coli* RecN to detect double-strand DNA breaks was

validated by comparison with *Bacillus subtilis* RecN-YFP expressed in the *E. coli thyA* mutant (*E. coli* RecN displayed the same extent of DSB foci as the well-characterized RecN from *B. subtilis* when expressed in *E. coli* as RecN-YFP fusions [54] (See Supplementary Fig. 9)). *recN-yfp* was introduced into *E. coli* strains by transduction to replace native *recN*. Log-phase cultures of *E. coli* were starved for thymidine, as above, to initiate TLD. Samples taken at various times were concentrated 10-fold by centrifugation (9,000 *g* for 20 s), mixed with 1/3 volume 1.5% low-melting-point agarose (FMC Corp., Philadelphia, PA) at 40°C, and immediately spread on a microscope slide.

For visualization of cells containing DNA breaks caused by exogenous H_2O_2, *recN-yfp* was cloned into plasmid pBAD18 between the *Eco* RI and *Hind* III sites to generate pBAD18-*recN-yfp*. For visualization of cells with single-strand DNA regions, the open reading frames of *ssb* (lacking a stop codon) and *yfp* were cloned into pBAD18 between the *Eco* RI and *Kpn* I sites and between the *Sal* I and *Hind* III sites, respectively, to generate pBAD18-*ssb-yfp*. Plasmid-expressed Ssb-YFP revealed single-strand DNA regions as fluorescent foci [55] (wild-type *ssb* was maintained in the chromosome). Recombinant plasmids were introduced separately into wild-type and *thyA* strains by bacterial transformation using electroporation. Thymine starvation, rifampicin treatment, and H_2O_2 treatment were as described above. Samples were removed after 20 min of peroxide treatment, washed with saline, and concentrated 10-fold by centrifugation.

Microscopy was performed with a Nikon Eclipse TS100 (Melville, NY) inverted microscope with filters for excitation and emission of YFP, and carboxy-H2DCFDA. Automated unbiased image acquisition was carried out with NIS Elements BR imaging software (Nikon Corp., Melville, NY).

Co-localization of DNA breaks with single-strand DNA regions

For visualization of DNA breaks occurring in single-strand DNA regions within the same cell, *recN-yfp* and *ssb-mCherry* were introduced into the genome of the *thyA* mutant to replace their native genes using bacteriophage P1-mediated transduction. After removal of thymidine, cells of strain 4496, grown to mid-log phase, were concentrated 10-fold by centrifugation (9,000 *g* for 20 s), and they were spotted onto an agarose pad on a microscope slide (prepared with fresh medium lacking thymidine, as described previously [56]). Slides with cells were immediately placed on a Zeiss Axiovert 200M microscope where they were kept at about 35 °C. DNA breaks (RecN-YFP), and single-strand DNA regions (Ssb-mCherry) in cells within the same field of view were recorded every 10 min.

Statistical considerations

All experiments were performed with at least three independent biological replicates. Three technical replicates were included for each sample point. Each value was presented as the mean value of the biological replicates, with standard deviation shown as error bars. At least 5 time points were chosen for each kinetic experiment to cover a wide range. *p*-values were not presented, since our data sought kinetic trends having greater than 10-fold differences in cell survival at multiple time points and qualitative differences in microscopic images and flow cytometry profiles.

Data availability and reagents

Data supporting the findings of this study are shown in the main text and in the supplementary information. They are available from the corresponding author upon request. No sequence, structure, or omics data required to be deposited in a public repository were generated in the study. Bacterial mutant strains and plasmids constructed in the work are listed in supplementary Table 1 and are available upon request.

Supplementary Material

Refer to Web version on PubMed Central for supplementary material.

Acknowledgments

References

1. Ahmad SI, Kirk SH, Eisenstark A. Thymine metabolism and thymineless death in prokaryotes and eukaryotes. Annu. Rev. Microbiol. 1998; 52:591–625. [PubMed: 9891809]

2. Cohen SS, Barner HD. Studies on unbalanced growth in *Escherichia coli*. Proc. Natl. Acad. Sci. U. S. A. 1954; 40:885–893. [PubMed: 16589586]

3. Smith DW, Hanawalt PC. Macromolecular synthesis and thymineless death in *Mycoplasma laidlawii* B. J. Bacteriol. 1968; 96:2066–2076. [PubMed: 4881702]

4. Sat B, Reches M, Engelberg-Kulka H. The *Escherichia coli mazEF* suicide module mediates thymineless death. J. Bacteriol. 2003; 185:1803–1807. [PubMed: 12618443]

5. Kunz BA, Glickman BW. Mechanism of mutation by thymine starvation in *Escherichia coli*: clues from mutagenic specificity. J. Bacteriol. 1985; 162:859–864. [PubMed: 3888966]

6. Fonville NC, Bates D, Hastings PJ, Hanawalt PC, Rosenberg SM. Role of RecA and the SOS response in thymineless death in *Escherichia coli*. PLoS Genet. 2010; 6:e1000865. [PubMed: 20221259]

7. Nakayama K, Kusano K, Irino N, Nakayama H. Thymine starvation-induced structural changes in *Escherichia coli* DNA. Detection by pulsed field gel electrophoresis and evidence for involvement of homologous recombination. J. Mol. Biol. 1994; 243:611–620. [PubMed: 7966286]

8. Pauling C, Hanawalt P. Nonconservative DNA replication in bacteria after thymine starvation. Proc. Natl. Acad. Sci. U. S. A. 1965; 54:1728–1735. [PubMed: 5326708]

9. Kuong KJ, Kuzminov A. Stalled replication fork repair and misrepair during thymineless death in *Escherichia coli*. Genes Cells. 2010; 15:619–634. [PubMed: 20465561]

10. Magner DB, et al. RecQ promotes toxic recombination in cells lacking recombination intermediate-removal proteins. Mol. Cell. 2007; 26:273–286. [PubMed: 17466628]

11. Fonville NC, Vaksman Z, DeNapoli J, Hastings PJ, Rosenberg SM. Pathways of resistance to thymineless death in *Escherichia coli* and the function of UvrD. Genetics. 2011; 189:23–36. [PubMed: 21705756]

12. Sangurdekar DP, et al. Thymineless death is associated with loss of essential genetic information from the replication origin. Mol. Microbiol. 2010; 75:1455–1467. [PubMed: 20132444]

13. Martin CM, Guzman EC. DNA replication initiation as a key element in thymineless death. DNA Repair (Amst). 2011; 10:94–101. [PubMed: 21074501]

14. Kuong KJ, Kuzminov A. Disintegration of nascent replication bubbles during thymine starvation triggers RecA- and RecBCD-dependent replication origin destruction. J. Biol. Chem. 2012; 287:23958–23970. [PubMed: 22621921]

15. Martin CM, Viguera E, Guzman EC. Rifampicin suppresses thymineless death by blocking the transcription-dependent step of chromosome initiation. DNA Repair (Amst). 2014; 18:10–17. [PubMed: 24742961]

16. Morganroth PA, Hanawalt PC. Role of DNA replication and repair in thymineless death in *Escherichia coli*. J. Bacteriol. 2006; 188:5286–5288. [PubMed: 16816201]

17. Hamilton HM, et al. Thymineless death is inhibited by CsrA in *Escherichia coli* lacking the SOS response. DNA Repair (Amst). 2013; 12:993–999. [PubMed: 24075571]

18. Khodursky A, Guzman EC, Hanawalt PC. Thymineless death lives on: new insights into a classic phenomenon. Annu. Rev. Microbiol. 2015; 69:247–263. [PubMed: 26253395]

19. Nakayama H, et al. Isolation and genetic characterization of a thymineless death-resistant mutant of *Escherichia coli* K12: Identification of a new mutation (*recQ1*) that blocks the RecF recombination pathway. Mol. Gen. Genet. 1984; 195:474–480. [PubMed: 6381965]

20. Nakayama K, Shiota S, Nakayama H. Thymineless death in *Escherichia coli* mutants deficient in the RecF recombination pathway. Can. J. Microbiol. 1988; 34:905–907. [PubMed: 2848620]

21. Courcelle J, Hanawalt PC. RecQ and RecJ process blocked replication forks prior to the resumption of replication in UV-irradiated *Escherichia coli*. Mol. Gen. Genet. 1999; 262:543–551. [PubMed: 10589843]

22. Ayusawa D, Shimizu K, Koyama H, Takeishi K, Seno T. Accumulation of DNA strand breaks during thymineless death in thymidylate synthase-negative mutants of mouse FM3A cells. J. Biol. Chem. 1983; 258:12448–12454. [PubMed: 6630193]

23. Kohanski MA, Dwyer DJ, Hayete B, Lawrence CA, Collins JJ. A common mechanism of cellular death induced by bactericidal antibiotics. Cell. 2007; 130:797–810. [PubMed: 17803904]

24. Dorsey-Oresto A, et al. YihE kinase is a central regulator of programmed cell death in bacteria. Cell Reports. 2013; 3:528–537. [PubMed: 23416055]

25. Zhao X, Drlica K. Reactive oxygen species and the bacterial response to lethal stress. Curr. Opin. Microbiol. 2014; 21:1–6. [PubMed: 25078317]

26. Dwyer DJ, Collins JJ, Walker GC. Unraveling the physiological complexities of antibiotic lethality. Annu. Rev. Pharmacol. Toxicol. 2015; 55:313–332. [PubMed: 25251995]

27. Demougeot C, et al. Cytoprotective efficacy and mechanisms of the liposoluble iron chelator 2,2'-dipyridyl in the rat photothrombotic ischemic stroke model. J. Pharmacol. Exp. Ther. 2004; 311:1080–1087. [PubMed: 15280435]

28. Beckman JS, Beckman TW, Chen J, Marshall PA, Freeman BA. Apparent hydroxyl radical production by peroxynitrite: implications for endothelial injury from nitric oxide and superoxide. Proc. Natl. Acad. Sci. U. S. A. 1990; 87:1620–1624. [PubMed: 2154753]

29. Hanawalt PC. Involvement of synthesis of RNA in thymineless death. Nature. 1963; 198:286.

30. Pinney RJ, Smith JT. R factor elimination during thymine starvation: effects of inhibition of protein synthesis and readdition of thymine. J. Bacteriol. 1972; 111:361–367. [PubMed: 4559728]

31. Lobritz MA, et al. Antibiotic efficacy is linked to bacterial cellular respiration. Proc. Natl. Acad. Sci. U. S. A. 2015; 112:8173–8180. [PubMed: 26100898]

32. Borisov VB, et al. Aerobic respiratory chain of *Escherichia coli* is not allowed to work in fully uncoupled mode. Proc. Natl. Acad. Sci. U. S. A. 2011; 108:17320–17324. [PubMed: 21987791]

33. Morimatsu K, Kowalczykowski SC. RecFOR proteins load RecA protein onto gapped DNA to accelerate DNA strand exchange: a universal step of recombinational repair. Mol. Cell. 2003; 11:1337–1347. [PubMed: 12769856]

34. Morimatsu K, Kowalczykowski SC. RecQ helicase and RecJ nuclease provide complementary functions to resect DNA for homologous recombination. Proc. Natl. Acad. Sci. U. S. A. 2014; 111:E5133–5142. [PubMed: 25411316]

35. Crooke ST, et al. Kinetic characteristics of *Escherichia coli* RNase H1: cleavage of various antisense oligonucleotide-RNA duplexes. Biochem. J. 1995; 312(2):599–608. [PubMed: 8526876]

36. Kitani T, Yoda KY, Ogawa T, Okazaki T. Evidence that discontinuous DNA-replication in *Escherichia coli* is primed by approximately 10 to 12 residues of RNA Starting with a purine. J. Mol. Biol. 1985; 184:45–52. [PubMed: 2411935]

37. Ogawa T, Okazaki T. Function of RNase H in DNA replication revealed by RNase H defective mutants of *Escherichia coli*. Mol. Gen. Genet. 1984; 193:231–237. [PubMed: 6319961]

38. Shimamoto T, Shimada M, Inouye M, Inouye S. The role of ribonuclease H in multicopy single-stranded DNA synthesis in retron-Ec73 and retron-Ec107 of *Escherichia coli*. J. Bacteriol. 1995; 177:264–267. [PubMed: 7528202]

39. Nakayama H, Hanawalt P. Sedimentation analysis of deoxyribonucleic acid from thymine-starved *Escherichia coli*. J. Bacteriol. 1975; 121:537–547. [PubMed: 1090581]

40. Lark KG. Evidence for the direct involvement of RNA in the initiation of DNA replication in *Escherichia coli* 15T. J. Mol. Biol. 1972; 64:47–60. [PubMed: 4552485]

41. Campbell EA, et al. Structural mechanism for rifampicin inhibition of bacterial rna polymerase. Cell. 2001; 104:901–912. [PubMed: 11290327]

42. Kobayashi S, Ueda K, Komano T. The effects of metal ions on the DNA damage induced by hydrogen peroxide. Agric. Biol. Chem. 1990; 54:69–76. [PubMed: 1368527]

43. Foti JJ, Devadoss B, Winkler JA, Collins JJ, Walker GC. Oxidation of the guanine nucleotide pool underlies cell death by bactericidal antibiotics. Science. 2012; 336:315–319. [PubMed: 22517853]

44. Cadet J, Ravanat JL, TavernaPorro M, Menoni H, Angelov D. Oxidatively generated complex DNA damage: tandem and clustered lesions. Cancer Lett. 2012; 327:5–15. [PubMed: 22542631]

45. Hanawalt PC, et al. Repair replication of DNA *in vivo*. Cold Spring Harb Symp Quant Biol. 1968; 33:187–194. [PubMed: 4891962]

46. Bendich AJ. The form of chromosomal DNA molecules in bacterial cells. Biochimie. 2001; 83:177–186. [PubMed: 11278067]

47. Hecht RM, Pettijohn DE. Studies of DNA bound RNA molecules isolated from nucleoids of *Escherichia coli*. Nucleic Acids Res. 1976; 3:767–788. [PubMed: 775442]

48. Kohanski MA, Dwyer DJ, Wierzbowski J, Cottarel G, Collins JJ. Mistranslation of membrane proteins and two-component system activation trigger antibiotic-mediated cell death. Cell. 2008; 135:679–690. [PubMed: 19013277]

49. Li L, et al. Ribosomal elongation factor 4 promotes cell death associated with lethal stress. MBio. 2014; 5:e01708. [PubMed: 25491353]

50. Davies BW, et al. Hydroxyurea induces hydroxyl radical-mediated cell death in *Escherichia coli*. Mol. Cell. 2009; 36:845–860. [PubMed: 20005847]

51. Bass DA, et al. Flow cytometric studies of oxidative product formation by neutrophils: a graded response to membrane stimulation. J. Immunol. 1983; 130:1910–1917. [PubMed: 6833755]

52. Dickinson BC, Chang CJ. Chemistry and biology of reactive oxygen species in signaling or stress responses. Nat. Chem. Biol. 2011; 7:504–511. [PubMed: 21769097]

53. Drummen GP, van Liebergen LC, Op den Kamp JA, Post JA. C11-BODIPY$^{581/591}$, an oxidation-sensitive fluorescent lipid peroxidation probe: (micro)spectroscopic characterization and validation of methodology. Free Radic. Biol. Med. 2002; 33:473–490. [PubMed: 12160930]

54. Kidane D, Sanchez H, Alonso JC, Graumann PL. Visualization of DNA double-strand break repair in live bacteria reveals dynamic recruitment of *Bacillus subtilis* RecF, RecO and RecN proteins to distinct sites on the nucleoids. Mol. Microbiol. 2004; 52:1627–1639. [PubMed: 15186413]

55. Youngren B, Nielsen HJ, Jun S, Austin S. The multifork *Escherichia coli* chromosome is a self-duplicating and self-segregating thermodynamic ring polymer. Genes Dev. 2014; 28:71–84. [PubMed: 24395248]

56. Skinner SO, Sepulveda LA, Xu H, Golding I. Measuring mRNA copy number in individual *Escherichia coli* cells using single-molecule fluorescent in situ hybridization. Nat. Protoc. 2013; 8:1100–1113. [PubMed: 23680982]
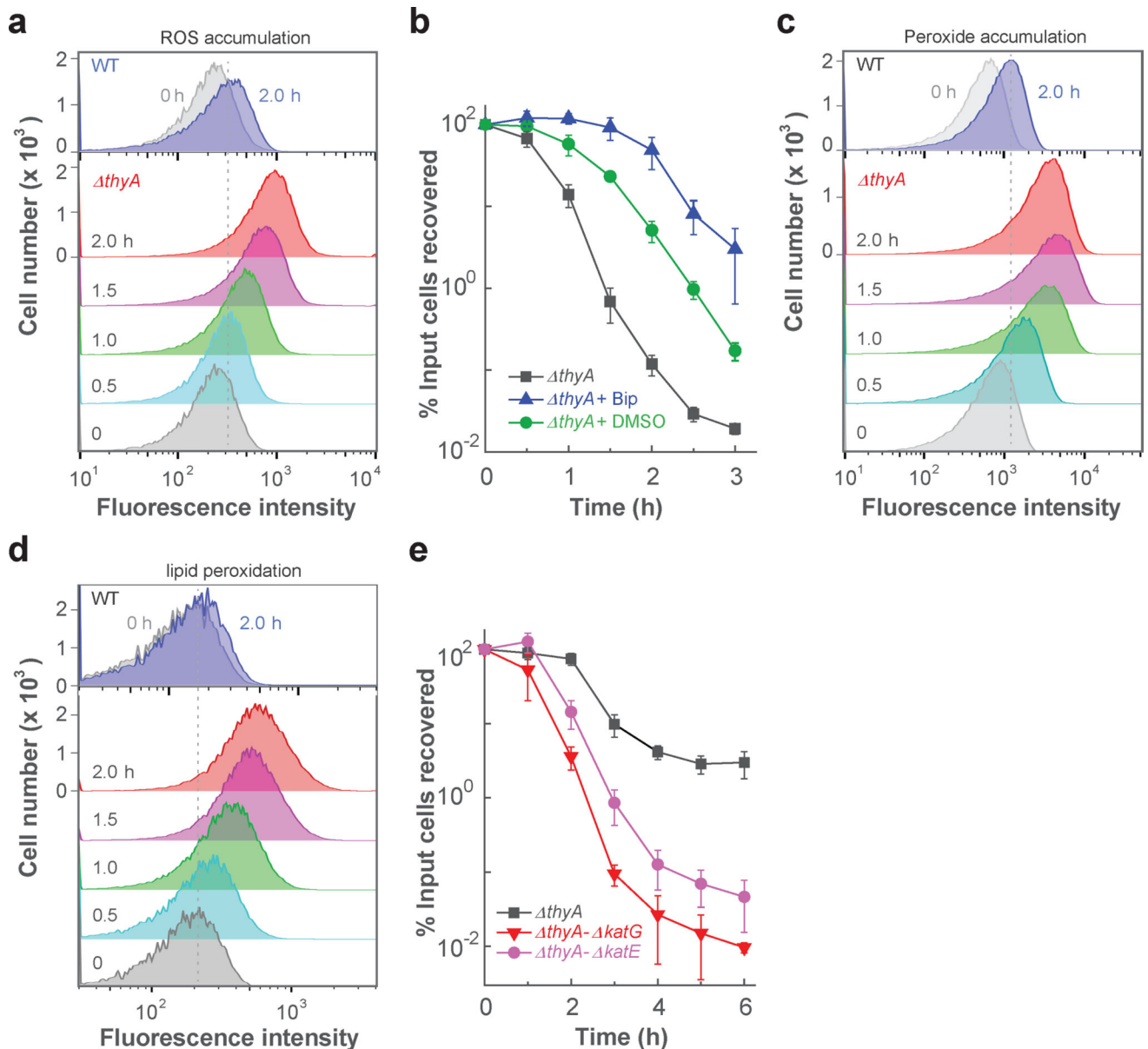
Figure 1. Association of ROS with TLD

a, ROS accumulation in a *thyA* mutant (strain 3640). T-starvation extended for the indicated times; ROS accumulation was monitored by flow cytometry using carboxy-H2DCFDA-mediated fluorescence. **b**, Inhibition of TLD. Rapid death of a thymidine-starved *thyA* culture (squares) was reduced by 2,2'-bipyridyl (Bip, triangles) or dimethyl sulfoxide (DMSO, circles), each at $0.5 \times$ MIC. Bipyridyl at $0.5 \times$ MIC slightly suppressed growth, but such growth inhibitory effects cannot account for the large protection from TLD (see Supplementary Fig. 14 for details). **c**, H_2O_2 accumulation during TLD. H_2O_2 was monitored at the indicated times after initiation of T-starvation by flow cytometry using Peroxy Orange-1-mediated fluorescence. **d**, Lipid peroxidation during TLD. Lipid peroxidation at the indicated times was detected by flow cytometry using C11-BODIPY-mediated fluorescence. **e**, Exacerbation of TLD by catalase/peroxidase deficiencies. Deletion

of *katG* (strain 3641) or *katE* (strain 3645), when present with a *thyA* mutation, decreased cell survival for samples taken at the indicated times during T-starvation. A nutrient-rich, defined medium (Hi-DEF Azure) was used for panels **a-d**; M9 minimal medium was used for panel **e** (see Supplementary Fig. 3d for KatG/E effects in Hi-DEF Azure medium). Panels **a, c** and **d** are representative for 3 independent experiments; data points are averages of three independent experiments in panels **b** and **e**; error bars represent standard deviation of the mean.
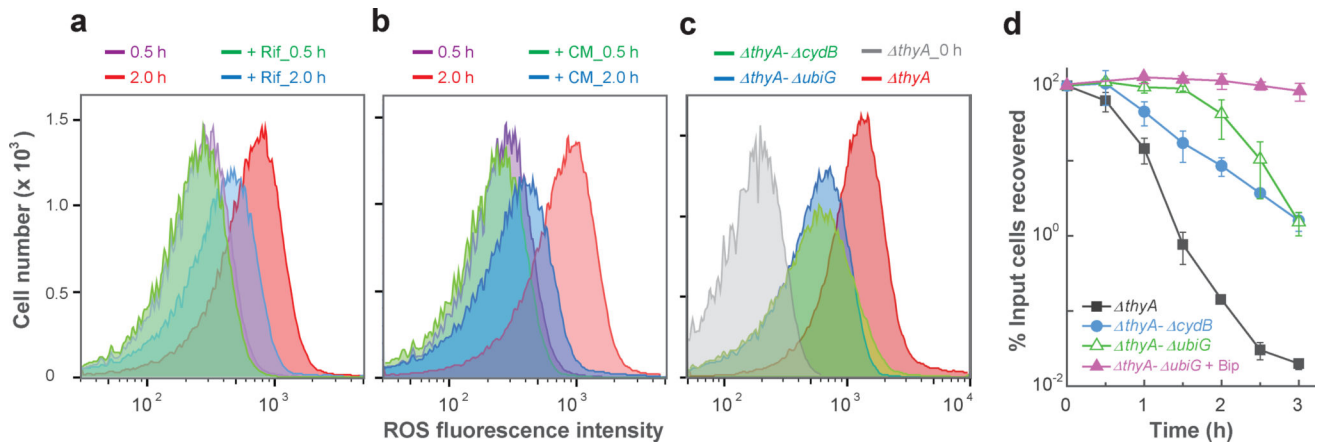
Figure 2. Suppression of ROS accumulation during T-starvation by rifampicin, chloramphenicol, or deficiencies in respiratory-chain genes

ROS was measured by flow cytometry as in Fig. 1a unless otherwise stated. Color coding for samples is shown above each panel. **a**, Effect of rifampicin. A *thyA E. coli* strain (3640) was treated with 50 μg ml^{-1} rifampicin when T-starvation was initiated; samples were removed for flow cytometry at the indicated times. **b**, Effect of chloramphenicol. Method was as in panel **a** except 40 μg ml^{-1} chloramphenicol replaced rifampicin. **c**, Effect of mutations in respiratory-chain genes on ROS. Cells were starved for thymidine for 3 h before samples were taken for flow cytometry. Bacterial strains were *thyA- ubiG* (3812), *thyA- cydB* (4012), and *thyA* (3640). **d**, Effect of mutations in respiratory-chain genes and bipyridyl on TLD. Cultures of double-deletion mutants (*thyA- ubiG, thyA cydB*) and *thyA- ubiG* plus bipyridyl (0.5 × MIC) were starved for thymidine; percent survival was determined at indicated times. Panels **a-c** are representative of 3 independent experiments; data points in panel **d** are averages for three independent experiments, with error bars representing standard deviation of the mean. No growth defect occurred when deficiencies in *cydB* and *thyA* were combined (Supplementary Fig. 14); a small inhibitory effect was observed with a *thyA- ubiG* double mutant and with addition of bipyridyl to a *thyA* mutant culture (Supplementary Fig. 14); however, substantial TLD was observed after a greater slowing of growth by incubation of the *thyA* single mutant at 30 °C (Supplementary Fig. 14), thereby arguing against the small growth inhibition by *ubiG* or bipyridyl being a major reason for protection from TLD.
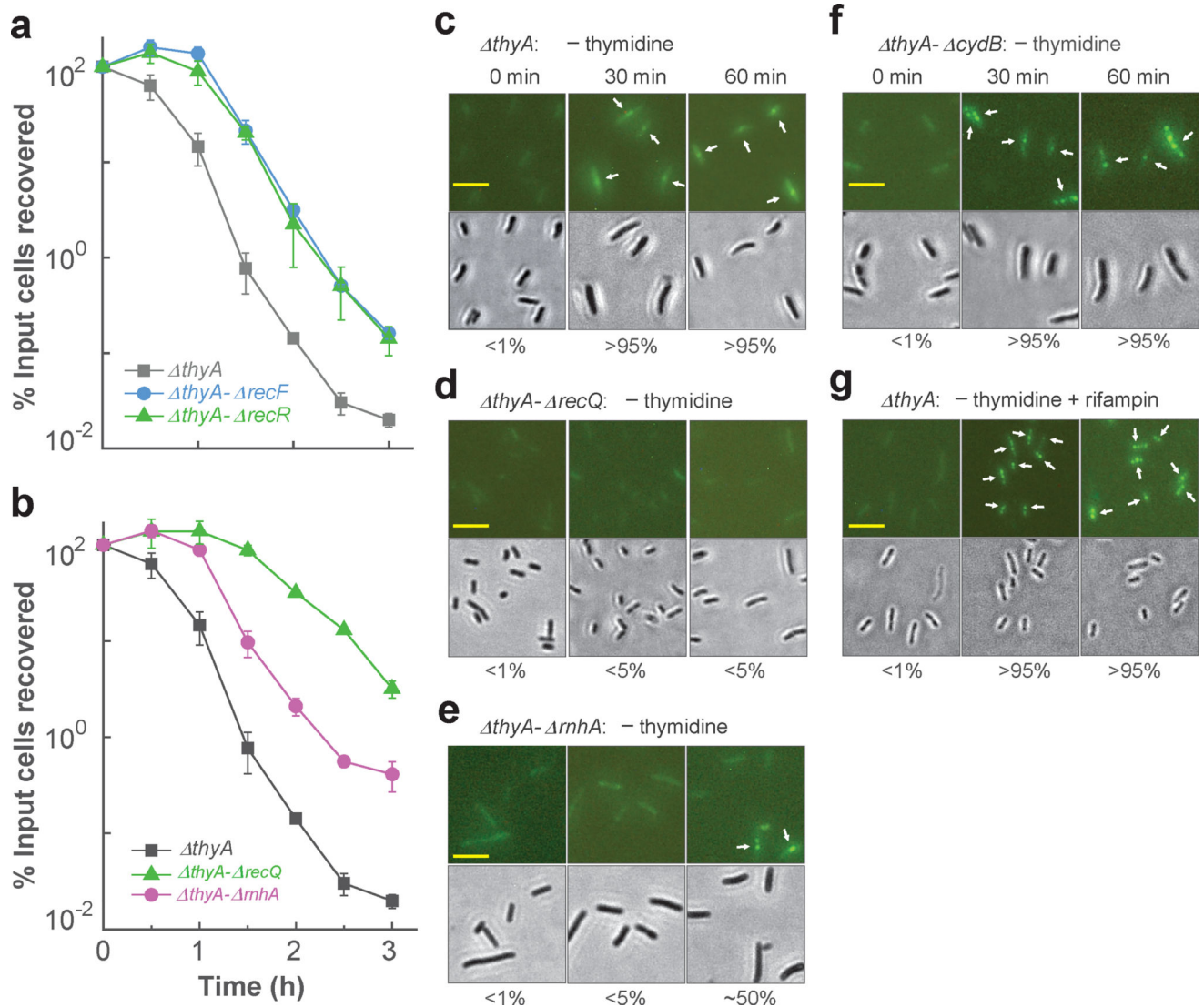
Figure 3. Single-strand DNA regions are necessary but insufficient for TLD

a, Effect of deficiencies of RecF or RecR. Mutants deficient in *thyA* and *recF* (strain 3711), *thyA* and *recR* (strain 3955), or only *thyA* (strain 3640) were starved for thymidine, and at the indicated times samples were taken for determination of percent survival. **b**, Effect of deficiencies in *recQ* and *rnhA*. Mutant strains were starved for thymidine, and at the indicated times percent survival was determined for *thyA* (strain 3640), *thyA- recQ* (strain 3952), and *thyA rnhA* (strain 3664). Data points in panels **a** and **b** are averages for three independent experiments; error bars represent standard deviation of the mean. **c**, Prevalence of *thyA* cells (strain 4313) with single-strand DNA regions. Fluorescent foci due to cellular binding of pre-induced Ssb-YFP to single-strand DNA regions (upper panels) are indicated by arrows. Lower panels: bright-field views of corresponding upper panels. Scale bar (in panels c-g) represents 10 μm; numbers under the panels indicate the prevalence of cells exhibiting fluorescent foci. **d**, Prevalence of *thyA- recQ* mutant cells with single-strand DNA regions. Methods were as in panel **c** but with strain 4335. **e**, Prevalence of *thyA- rnhA* mutant cells exhibiting single-strand DNA regions. Methods were as in panel

c but with strain 4389. **f**, Prevalence of *thyA- cydB* mutant cells exhibiting single-strand DNA regions. Methods were as in panel **c** but with strain 4012. **g**, Effect of rifampicin on prevalence of cells having single-strand DNA. Rifampicin (50 µg ml^{-1}) was added to the *thyA* culture (strain 4313) at the time T-starvation was initiated. Methods were as in panel **c**. Similar results were observed in 3 independent experiments for panels **c-g**; 200 cells for each group were randomly selected for analysis of generation of single-strand DNA regions.
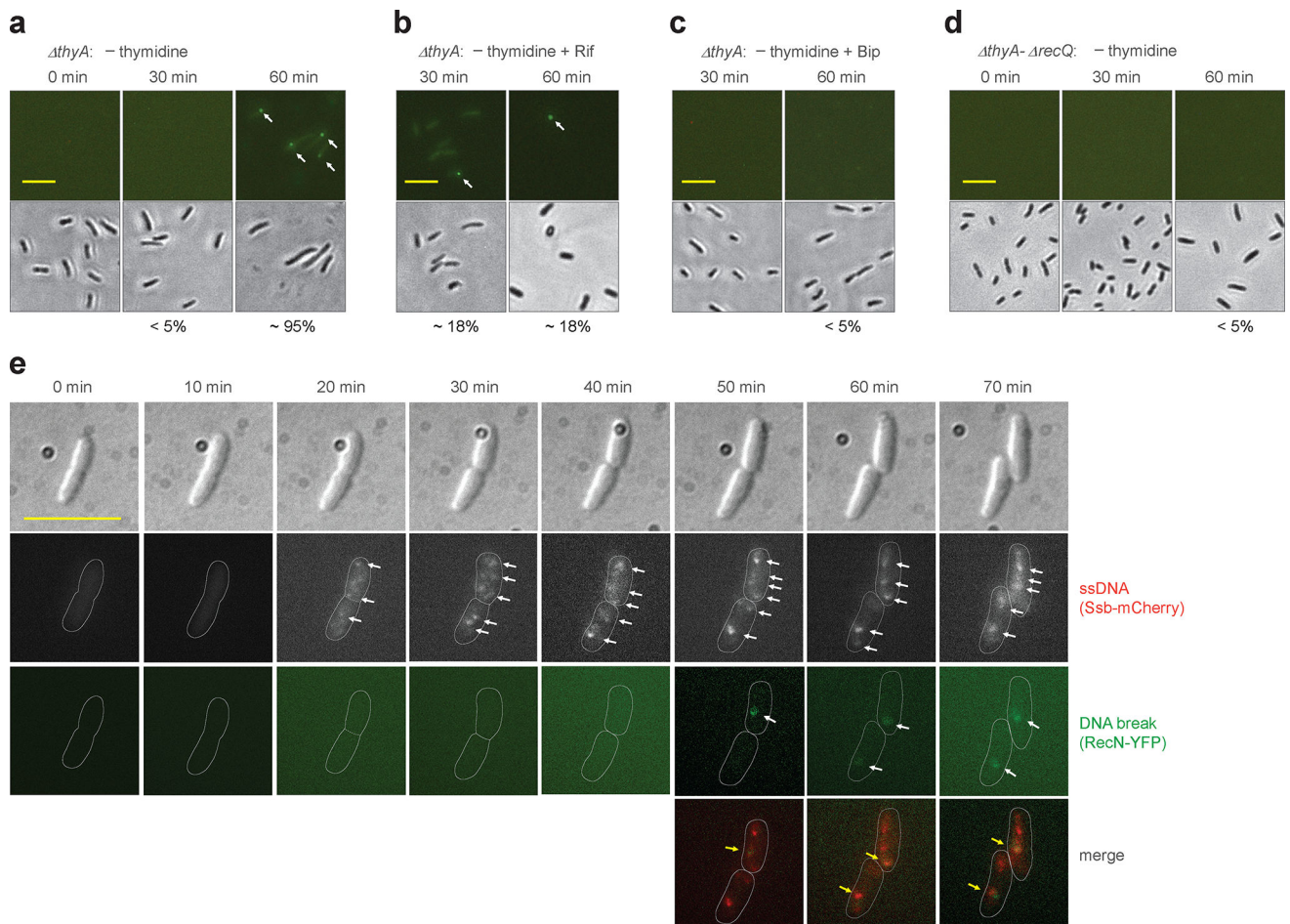
Figure 4. Double-strand DNA breaks associated with TLD

a, Prevalence of *thyA* cells with double-strand DNA breaks during T-starvation. Strain 4258 (*recN-yfp*) was pre-induced with 0.1% arabinose for 2.5 h and then starved for thymidine for the indicated times followed by examination by fluorescence (upper panels) or bright field microscopy (lower panels). Arrows indicate fluorescent foci. Scale bar (in all panels) represents 10 μm. Prevalence of cells with at least one fluorescent focus is shown as percentage below panels. **b**, Effect of rifampicin on presence of DNA breaks during T-starvation. Methods were as in panel **a** except rifampicin (50 μg ml^{-1}) was added immediately after thymidine removal. **c**, Effect of 2,2'-bipyridyl (Bip) on presence of DNA breaks during T-starvation. Methods were as in panel **a** except for addition of $0.5 \times$ MIC Bip immediately after thymidine removal. **d**, Effect of *recQ* on formation of DNA breaks during T-starvation. Methods were as in panel **a** but with strain 4262 (*thyA- recQ*). **e**, Co-localization of DNA breaks and single-strand DNA regions during T-starvation. Ssb-mCherry was constitutively expressed under the native *ssb* promoter in the chromosome of a *thyA recN-yfp* mutant (strain 4315). Two typical thymidine-starved cells are shown for appearance of DNA breaks in the single-strand DNA region. Arrows indicate fluorescent foci. About 60% of DNA breaks (green RecN-YFP foci, n = 30) co-localized with regions of single-strand DNA. All images are typical from pictures obtained from 3 independent experiments. For panels **a-d**, 200 cells for each group were randomly selected for analysis of

generation of DNA breaks. Detection of double-strand DNA breaks by *E. coli* RecN was verified by finding the same results with *Bacillus subtilis* RecN expressed in *E. coli* (see Supplementary Fig. 9).
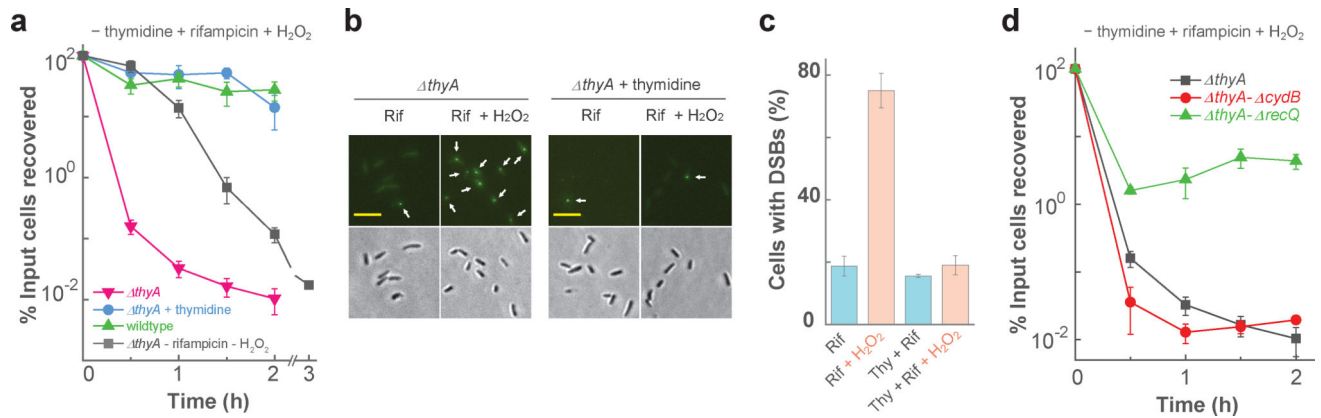
Figure 5. Conversion of single-strand DNA regions into lethal breaks by exogenous ROS

a, Exogenous H_2O_2 reduced survival of rifampicin-treated cells starved for thymidine. Rifampicin was added at the time of thymidine removal. At the indicated times after thymidine removal, H_2O_2 was added to 3.5 mM (unless otherwise indicated) for 20 min before sampling for survival. Squares, *thyA* (strain 3640) without rifampicin or H_2O_2 treatment; circles, *thyA* (strain 3640) incubated with 200 μg ml^{-1} thymidine plus rifampicin and H_2O_2 treatment; triangles, wild-type (strain 3001) plus rifampicin and H_2O_2 treatment; inverted triangles, *thyA* (strain 3640) plus rifampicin and H_2O_2 treatment. **b**, Exogenous H_2O_2 increased the prevalence of cells exhibiting DNA breaks. Plasmid-borne RecN-YFP was pre-induced by 0.1% arabinose for 2.5 h during growth of strain 4282 before removal of thymidine. H_2O_2 (3.5 mM) was added to cultures after 30-min rifampicin treatment and T-starvation. Upper panels show fluorescence after 20 min H_2O_2 treatment; lower panels are corresponding bright-field views. Scale bar, 10 μm. Microscopy results are representative of three independent experiments. **c**, Prevalence of cells with double-strand breaks generated by exogenous H_2O_2 administered as in panel **b**. Abbreviations: DSB double-stranded DNA break; Rif, rifampicin; Thy, thymidine. Number of cells examined for the four groups (Rif, Rif + H_2O_2, Thy + Rif, and Thy + Rif + H_2O_2) were 1040, 640, 460, and 1190 cells, respectively. Data from three independent experiments were used for analysis. **d**, Effect of *recQ* and *cydB* deficiencies on survival of rifampicin-treated, thymidine-starved *thyA* cells when exposed to exogenous H_2O_2. H_2O_2 treatment was as in panel **a**. Squares, *thyA* (strain 3640); circles, *thyA-cydB* (strain 4012); triangles, *thyA-recQ* (strain 3952). Error bars in panels **a, c** and **d** represent standard deviation of the mean determined from three independent experiments.
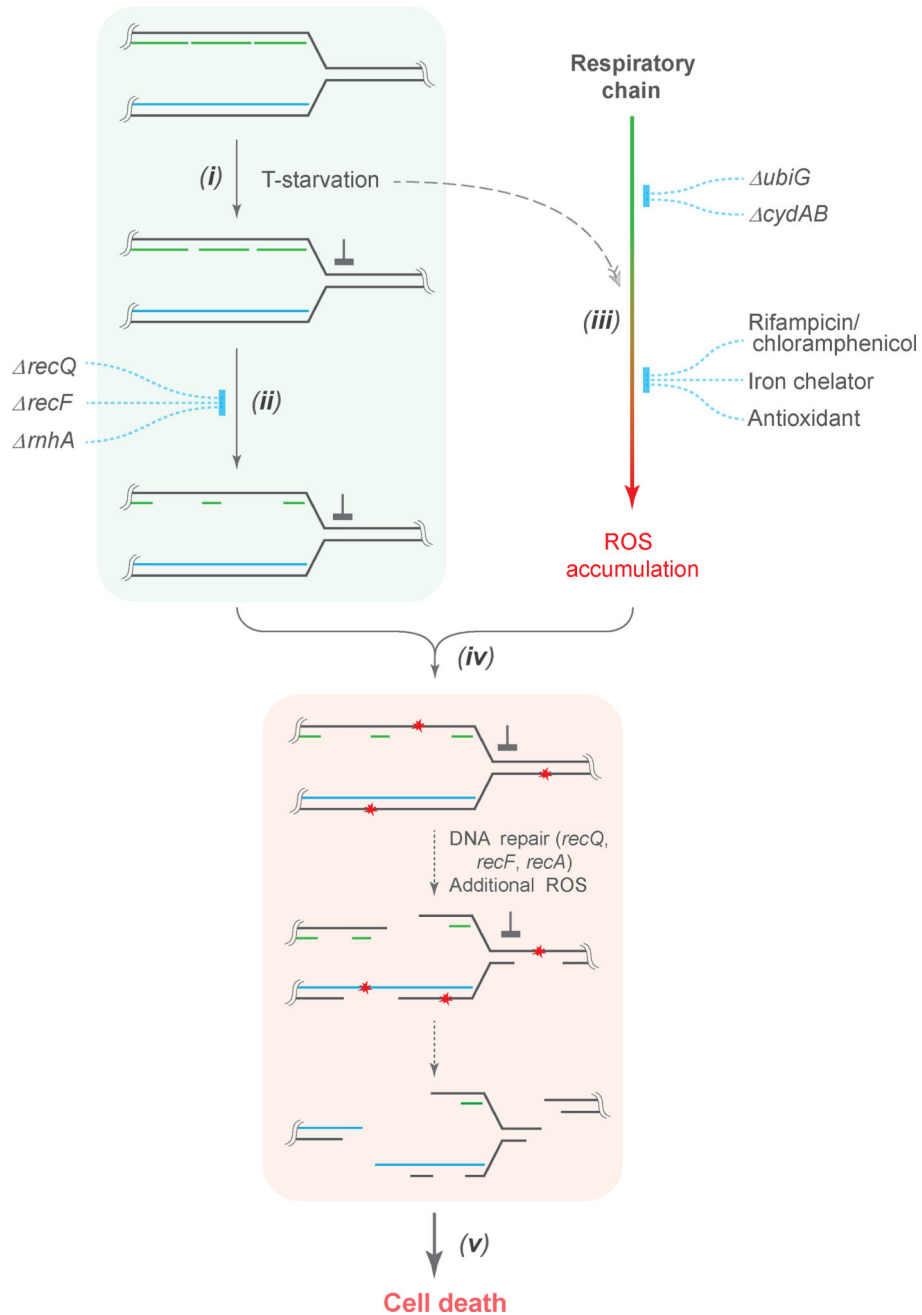
Figure 6. Scheme describing ROS-mediated conversion of single-strand DNA regions into lethal DSBs during TLD

(**i**) When growing cells are starved for thymine, DNA replication forks stall; they then advance slowly by recruiting thymine from degraded DNA. (**ii**) Single-strand DNA regions, located in the lagging strands behind replication forks and at sites of single-strand lesion repair, enlarge due to attempted repair in the absence of dTTP. The number and size of single-strand DNA regions increase due to DNA-damage-repair systems (RecQ/RecFOR) and due to degradation of RNA from RNA-DNA hybrids (RnhA). (**iii**) T-starvation triggers accumulation of intracellular ROS as byproducts of respiration. Disruption of the respiratory

chain by deletion of *ubiG* or *cydAB* decreases ROS generation. Addition of RNA or protein synthesis-inhibiting agents (rifampicin or chloramphenicol) inhibits cell respiration, thereby suppressing the ROS surge. ROS accumulation is also inhibited by the presence of Fe^{2+} chelators, such as 2,2'-bipyridyl, or antioxidants, such as DMSO. These ROS-inhibiting agents have little effect on expansion of single-strand DNA regions (**iv**) DNA is attacked by ROS, especially hydroxyl radical. When ROS attack occurs in single-strand DNA regions, DSBs arise; ROS-mediated attack of double-strand DNA leads primarily to single-strand lesions, which could be expanded into large single-strand regions by abortive DNA repair in the absence of dTTP. (**v**) Extensive DNA breakage results in cell death, with deficiencies in DSB repair exacerbating TLD[11]. Induction of SOS/*sulA*, which may occur at multiple steps in the scheme, can lower the ability of cells to resume growth after thymine becomes available[6].